Supplemental

Adsorption of water on graphene/Ru(0001) - an experimental ultra-high vacuum study

A. Chakradhar, U. Burghaus

Department of Chemistry and Biochemistry,
North Dakota State University, Fargo, USA

www.uweburghaus.us

Generic list of acronyms and abbreviations

AFM	atomic force microscopy
CMA	cylindrical mirror analyzer
CNTs	carbon nanotubes
CVD	chemical vapor deposition
DFT	density functional theory
EBL	electron beam lithography
EDX/EDS	energy dispersive X-ray spectroscopy
GC	gas chromatograph
HDS	hydrodesulfurization
HREELS	high resolution electron energy loss spectroscopy
IF	inorganic fullerene-like nanoparticles
LEED	low energy electron diffraction
MCS	Monte Carlo simulations
NDSU	North Dakota State University
NT	nanotubes
NP	nanoparticles
PNNL	Pacific Northwest National Laboratory
PVD	physical vapor deposition
SEM	scanning electron microscopy
STM	scanning tunneling microscopy
TEM	transmission electron microscopy
TiNTs	TiO_2 nanotubes
TDS	thermal desorption spectroscopy
TOF	time of flight spectroscopy
UHV	ultra-high vacuum
UPS	ultraviolet photoelectron spectroscopy
UV	ultraviolet
XPS	X-ray photoelectron spectroscopy

Sample characterization and fabrication

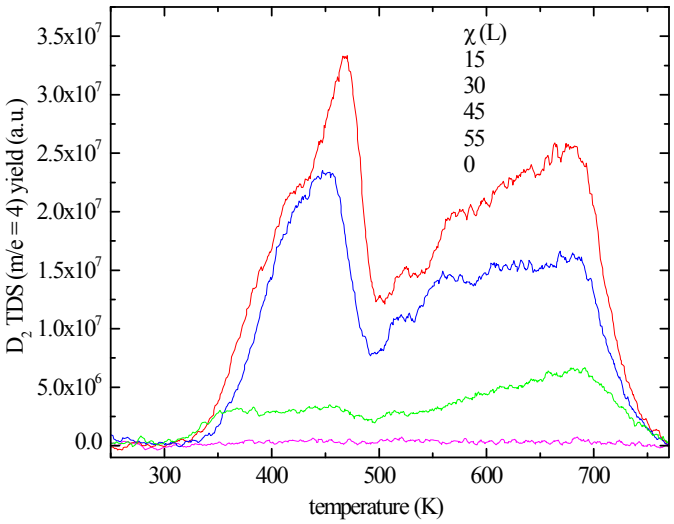

Fig. S1: D_2 TDS after exposure of C_6D_6 on Ru(0001). The forming graphene patches block adsorption sites for hydrogen on Ruthenium, i.e., the D_2 intensity decreases. χ is the exposure of benzene in Langmuir. (See ref.[1] for details.)

Defect density, D_2 TDS. For the PVD of graphene, we did follow a "synthesis" procedure described in ref.[1]. Accordingly, benzene adsorption desorption cycles are monitored by measuring the D_2 signal. Deuterated benzene is used to discriminate against a possible hydrogen background. **Fig. S1** shows that the D_2 TDS signal vanishes when the graphene layer is formed. The D_2 signal disappears since only Ru sites can decompose the benzene. The remaining D_2 signal may therefore be used to estimate the defect density of the epitaxial graphene layer. According to **Fig. S1,** that defect density amounts to <1.7%, when integrating the TDS curves.

Single layer graphene is formed on Ruthenium. The advantage of using Ruthenium as a support for this model study is that we can rule out *a priori* double layer graphene. The growth mechanism of graphene on Ruthenium does not allow for double layer formation. We use a

physical vapor deposition technique. (Note that in most engineering type studies commercial samples were used which where made by chemical vapor deposition. That process is cheap, but probably not ideal for a model study.) Briefly, the clean ruthenium sites catalyze the bond breaking in hydrocarbons. The so formed carbon poisons the catalyst. Thus, catalyst activity and graphen growth stops once all ruthenium sites are covered with single carbon atoms. The graphene growth on ruthenium is self-terminating. Double layers cannot be formed. The late W. Goodman (and others[2]) collected scanning tunneling microscopy images of these samples.[3-5] Accordingly, indeed a single carbon layer is formed on Ruthenium. Furthermore, graphene growth as a carpet over step edges and defects of the support.[3-5] Thus, a single layer of single crystalline graphene is formed giving rise, for example, to the well-known More LEED pattern (see our Fig. S3). In addition, we use deuterated benzene as the carbon source and monitor the D_2 signal while forming graphene. That D_2 TDS signal basically disappears below the detecting limit which is of the order of 1% of a monolayer. (see our Fig. S1 and also ref.[1]) Thus, the defect density of the graphene layer on Ruthenium is extremely small. Two layer islands cannot form since Benzene does not dissociate on graphene/HOPG.[6] Supposingly, carbon binds stronger to Ruthenium than to carbon. Therefore, formed graphene will not diffuse on top of graphene. At least islands on top of graphene were not seen in STM.[3-5] In fact, the rather large annealing temperatures are required to induce carbon diffusion (rather than benzene bond activation) on the ruthenium support forming the closed layer of graphene.

In summary, Benzene dissociates only on clean ruthenium sites, depositing carbon atoms and desorbing D_2 into the gas phase. Benzene dissociation stops once all Ru atoms are covered with Carbon atoms. Similarly, D_2 desorption stops once the surface is covered with carbon. The LEED pattern indicates single crystalline graphene.)

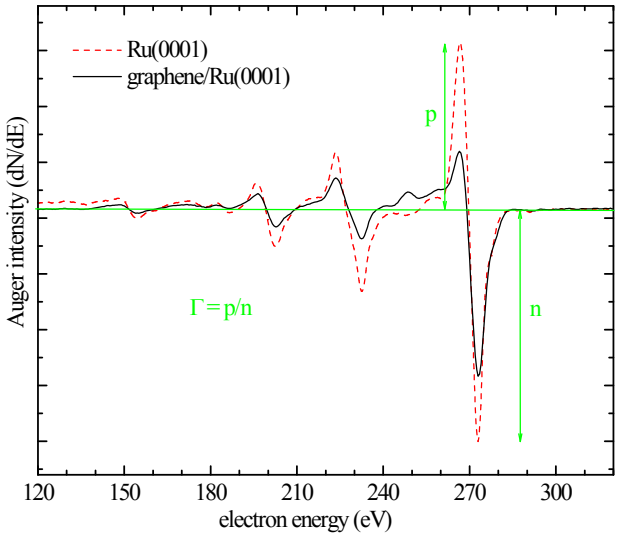

Fig. S2: Auger electron spectra of clean Ru(0001) and graphene/Ru(0001). The intensity of the carbon AES line can be used to monitor graphene formation, see e.g. ref.[5] The AES ratios obtained here are 0.74 for Ru(0001) and 0.34 for graphene/Ru(0001).

AES data. Similarly the C AES ratio can be used to characterize the graphene layer as illustrated in **Fig. S2**. See ref.[1] for details. The AES ratios obtained for a clean Ruthenium support and the graphene layer are consistent with prior STM studies (see refs in ref.[5]).

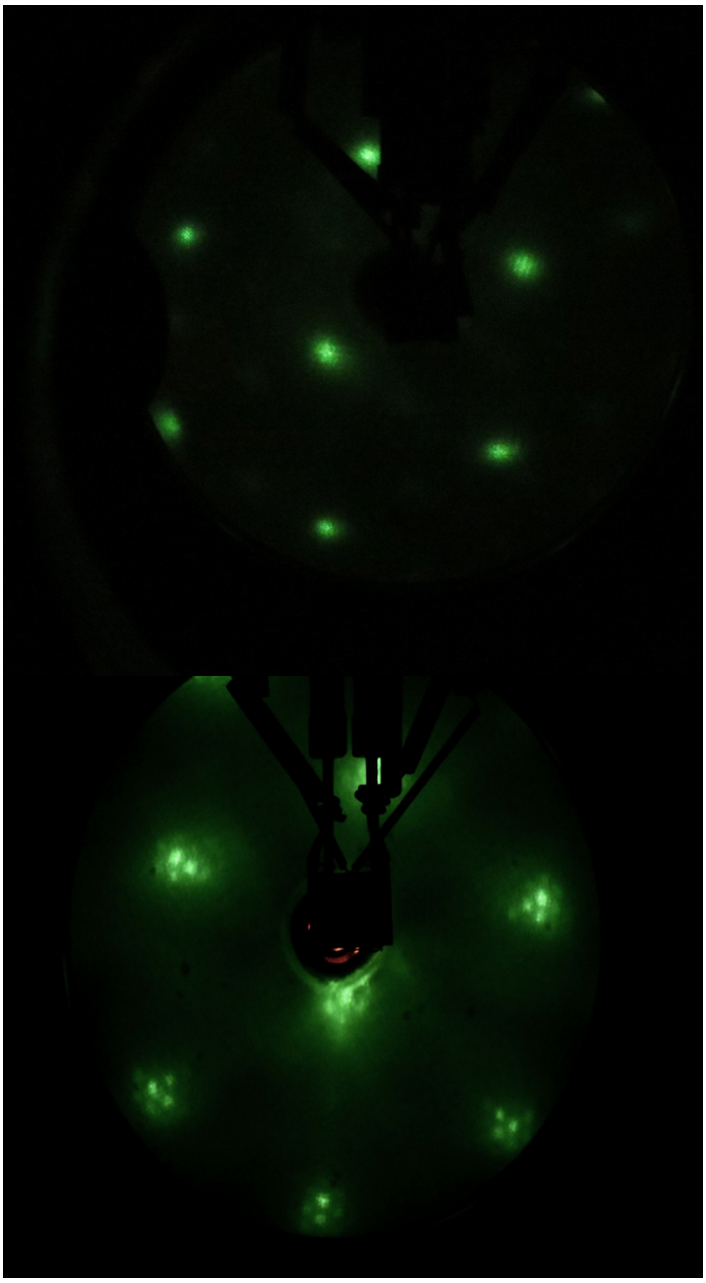

Fig. S3. Top) LEED of Ru(0001) from ref [Chemical Physics Letters, 590 (2013) 146 - 152] **Bottom)** LEED of graphene/Ru(0001) fabricated used the same technique from ref [Chemical Physics Letters, 590 (2013) 146 - 152]. Note the satellite peaks caused by the graphene layer.

LEED. Fig. S3 shows the LEED images of Ruthenium and graphene/ruthenium samples made in our lab using the same procedure. The satellite peaks indicate the formation of graphene.

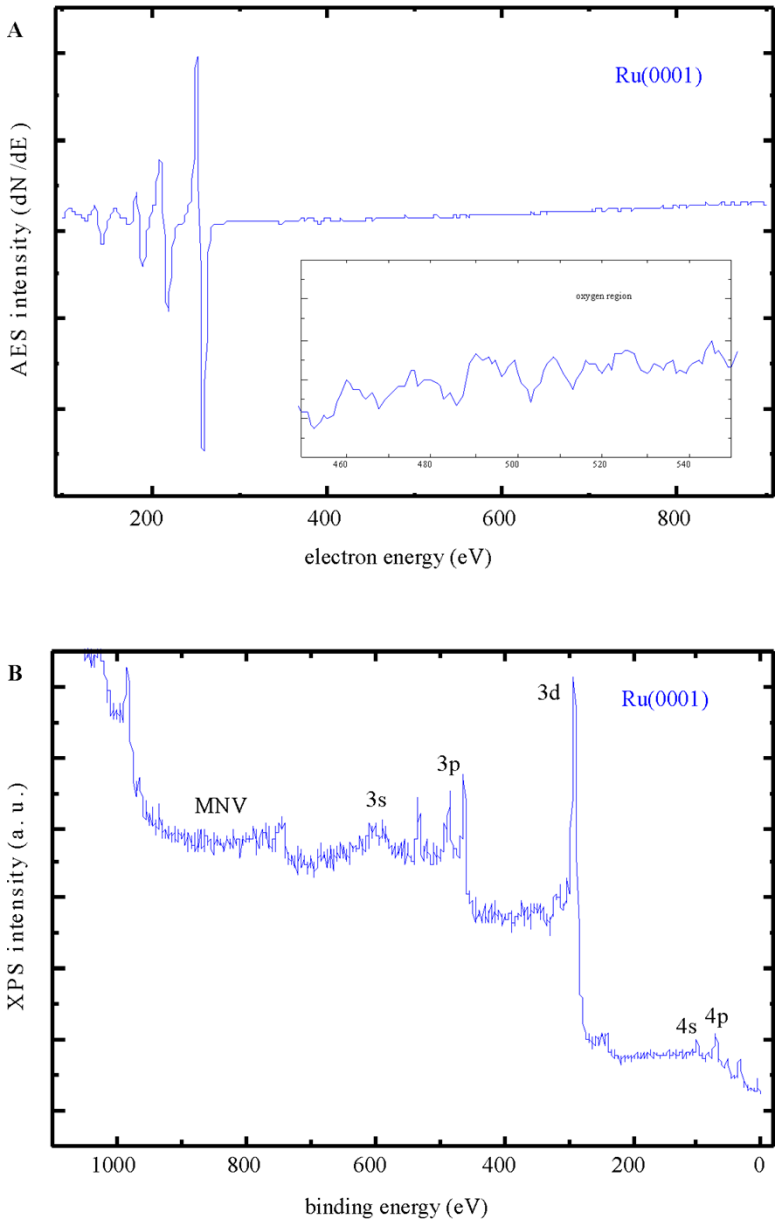

Fig. S4: XPS and AES survey spectra of the clean Ru(0001) support.

Fig. S4 and **Fig. S5** depict further AES and XPS data of the clean and graphene covered support.

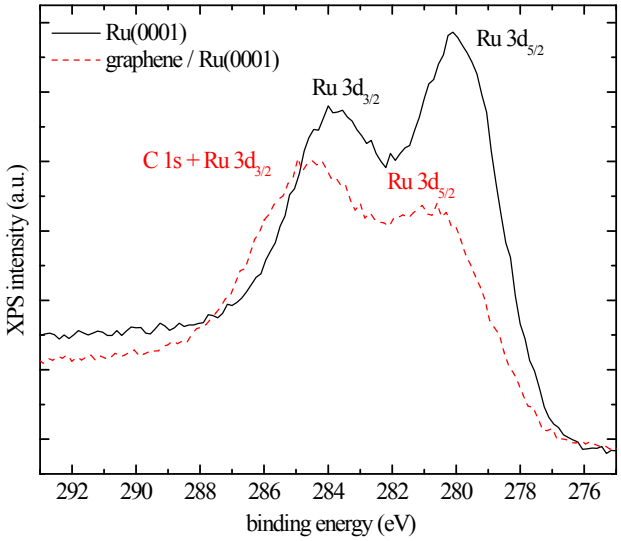

Fig. S5: XPS of Ru(0001) and graphene/Ru(0001) fabricated using the same technique from ref [Chemical Physics Letters, 590 (2013) 146 - 152].

XPS. Unfortunately, for Ruthenium, XPS Ruthenium lines overlap with the carbon line (Fig. S5). Therefore, the width of the C1s XPS peaks is rather large. As a result, AES or XPS peak ratios are used to characterize graphene on Ruthenium.[1] The peak broadening is not related to the adsorption of functionalities.

Why we cannot use Raman spectroscopy. The sole purpose of the present study is characterizing the intrinsic properties of graphene for water adsorption as good as possible. The only way to do so, in our opinion, is using an ultra-high vacuum (UHV) setup. If these intrinsic features are highly relevant for applications or not, is perhaps a different concern, but the intrinsic properties of graphene cannot be characterized in air. For example, 30 min air exposure results in a loss of the LEED pattern, taking AES of a 30 min are exposed sample shows huge amounts (in surface science terms) of amorphous carbon deposits; see ref.[1]

Despite the unfortunate fact that we don't have a Raman system, all Raman spectrometers we are aware of operate in air.[7] Therefore, the sample would need to be removed from the UHV

chamber and transferred to a Raman system. What we would find then is a dirty graphene sample, similarly to our AES data in ref.[1]-supplemental. This would not provide any additional information (and we don't have a Raman spectrometer).

Similar concerns hold true for any kind of electron/optical microscopy inspection of the samples. Either we just find a dirty sample or the sensitivity of these techniques is too low.

In addition, prior works from other groups (using the same preparation techniques) show high quality graphene/Ru samples.[2-5]

Sample cleanliness and stability

The advantage of UHV surface science studies is the ultra-high vacuum environment that keeps samples clean. At ambient pressure, samples are generally covered with impurities within milli seconds. In a prior project we examined the cleanliness of graphene/Ru(0001) samples at ambient pressure, see supplemental to ref.[1] Exposing that sample to air for more than 30 min resulted in irreversible destruction of the graphene layer, as judged by AES and LEED. Different samples may behave differently. For example, in some cases flashing samples at UHV to great temperatures may restore the pristine state.[8] That procedure did, however, not work with our graphene/Ru(0001) samples, i.e., once the graphene was degraded, the carbon layer had to be sputtered off and a fresh graphene sample had to be grown. Fresh UHV grown graphene/Ru(0001) samples were regularly flashed to 1300 K in UHV. Base pressure in our UHV chamber amounts to $<2\text{x}10^{-10}$ mbar.

Water intercalation was indeed reported in the literature, as far as we know, mostly for multi-layer graphene.[9] Besides that we don't form multilayer graphene on Ruthenium, a water intercalation would change the morphology of the graphene layer significantly. (Graphene is

heavily fragmented according to ref.[9] Clean Ruthenium sites would form.) Therefore, it is expected that also the TDS data would change with the water exposure and/or the samples history. We have not recognizes changes in the TDS data over time. The TDS curves were well reproducible over weeks. (e.g. Fig. 1 and Fig. S7 were collected from the same graphene layer.) In addition, note that water TDS from clean Ruthenium looks different than water TDS from grahene/Ruthenium.

Additional data

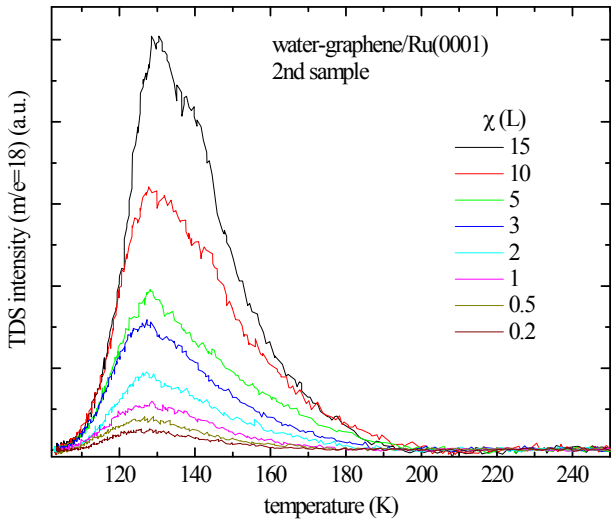

Fig. S6: water UHV TDS of graphene/Ru(0001). Data for a second graphene sample.

TDS data of a 2nd graphene/ruthenium sample are shown in **Fig. S6**. The data in Fig. 1 and **Fig. S6** are very similar. Water was dosed by backfilling the vacuum chamber. A small shoulder is probably evident for large exposures at the high temperature side of the curves which is likely caused by readsorption effects.

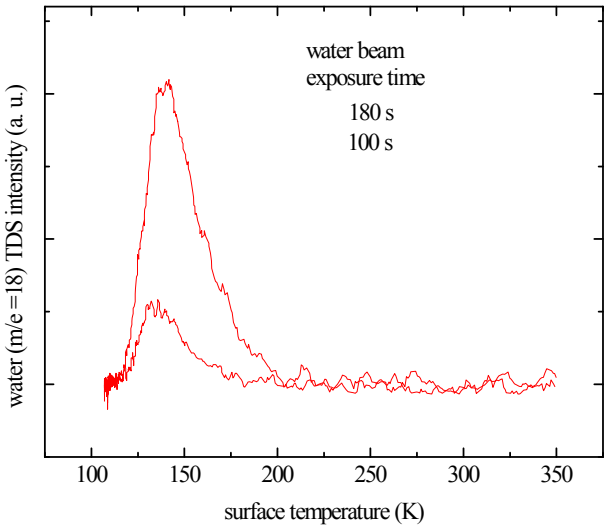

Fig. S7: water UHV TDS of graphene/Ru(0001). Water was dosed with a molecular beam system.

Fig. S7 depicts TDS curves where water was dosed by a molecular beam system. Also in this case very similar TDS curve shapes were obtained. Therefore, we rule out that readsorption effects and pumping curve effects obscured the TDS curve shapes (Fig. 1, Fig. S7) for water – graphene/Ru(0001).

Data analysis

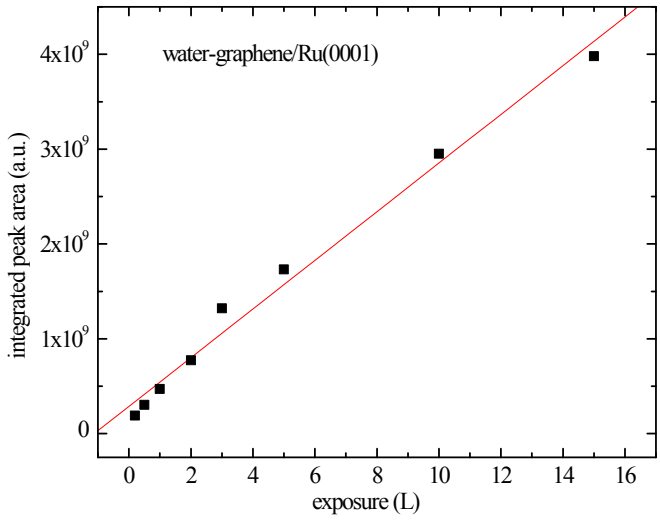

Fig. S8: analysis of the water UHV TDS curves of graphene/Ru(0001).

Fig. S8 shows that the total TDS peak area increases linearly with the exposure. As expected for a condensation process with an adsorption probability of one.

Data analysis for Fig. 2 of the draft (binding energy)

Fig. 2 in the main document was obtained using the following data analysis procedure. For strictly 0th order kinetics the desorption rate, k, is simply described by an Arrhenius equation, according to:

$$k = k_d[A_{ads}]^0 = k_d;$$

$$\mathrm{k_d} = \nu_d e^{-E_b/RT};$$

$$\ln(k_d) = \ln(\nu_d) - E_b / R\frac{1}{T} \text{ or}$$

$$\ln(k_d) = \ln(\nu_d) - E_b / k_b\frac{1}{T}$$

With k_d as the desorption rate coefficient, ν, the preexponential coefficient, E_b, the binding energy (here sublimation energy of water), T, the surface temperature, $[A_{ads}]$ or Θ, the adsorbate coverage/concentration, R, the gas constant, k_b the Boltzmann constant. Or, we could also write

$$\beta \frac{d\Theta}{dT} = k_d = \nu e^{-E/RT}$$
$$\beta r = \nu e^{-E/RT}$$
$$r = \nu/\beta \, e^{-E/RT}$$
$$\ln(r) = \ln(\nu/\beta) - E / RT$$

Taking the heating rate, β, into account. TDS measure the pressure of the desorbing adsorbates, or, equivalent to that, the change of coverage (surface concentration) which is given by dΘ/dT. The change of coverage with temperature equals the desorption rate, r. The desorption rate is proportional to the measured pressure (i.e. the TDS peak intensity).

Fig. 2 shows this kind of simple data analysis. The TDS peak positions (in Kelvin) are plotted vs. the logarithm of the desorption rate (TDS peak intensity). The TDS data set of Fig. 1 was used. The slope of the fit line gives one the heat of sublimation of water (see equations above). In doing so, numerical values very close to the heat of sublimation of water were obtained, another indication for simple condensation kinetics of water on graphene.

Computer simulation of standard kinetics

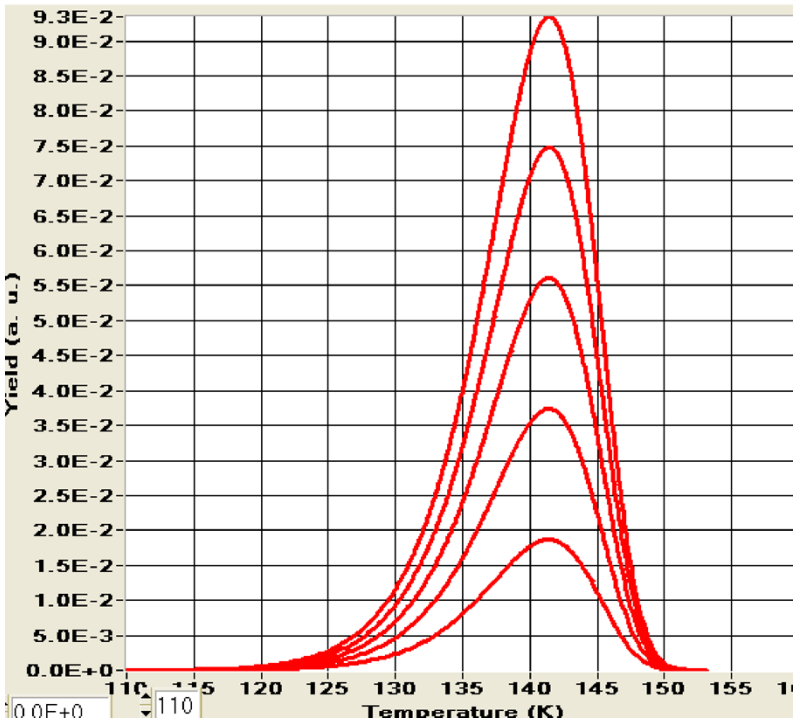

Fig. S9: Computer simulation of typical low temperature 1st order kinetics. The high temperature edge is steeper than the low temperature rise, opposite to water on graphene/Ru. (Coverages 0.2, 0.4, 0.6, 0.8, 1.0 ML; binding energy 40 kJ/mol and preexponential $1x10^{14}$/sec; heating rate 1.4 K/s).

Fig. S9 and Fig. S10 depict computer simulations of traditional 1st and 2nd order kinetics. As evident, the curve shapes are very different than those observed for graphene/Ruthenium. **Fig. S11** shows experimental data of our group, collected with the same setup, which show 0th order kinetics for a strictly hydrophobic system. The water graphene/Ru(0001) data may perhaps be fitted with a kinetics model. However, it appears that coverage dependent kinetics would be required to reproduce the actual shape of the TDS curves.

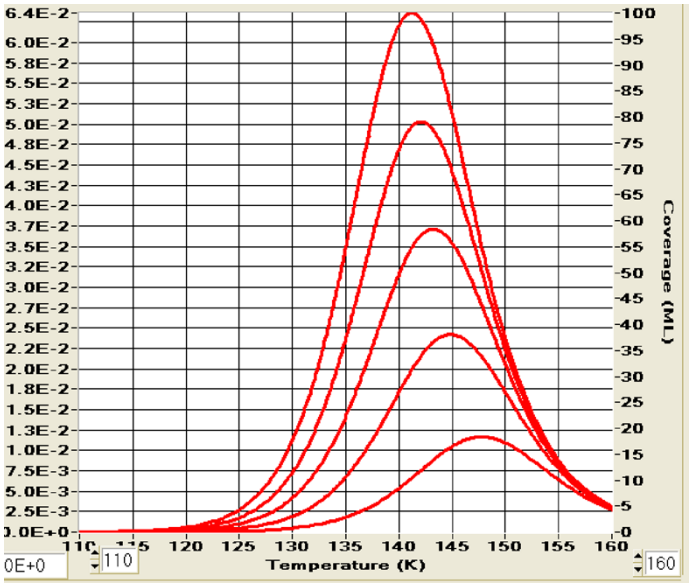

Fig. S10: Computer simulation of a typical low temperature 2nd order kinetics. The peaks shift to the left (with increasing exposure), opposite to graphene/Ru. (Same parameters as above.)

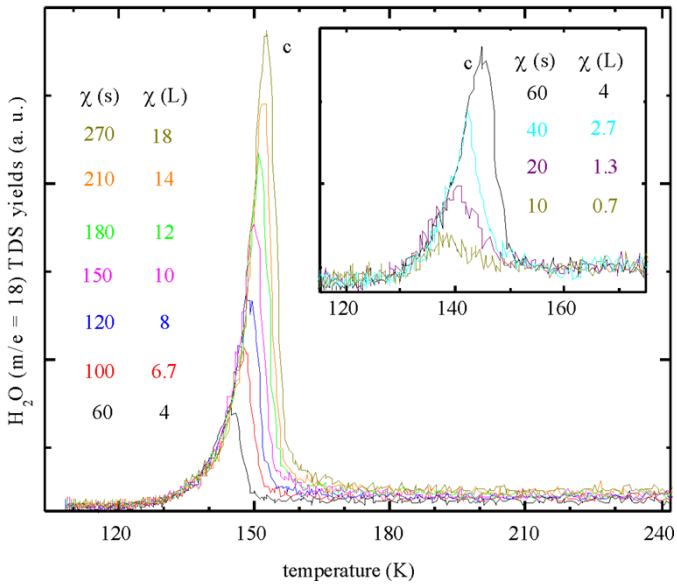

Fig. S11: Example of a strict 0th order kinetics data set – see *Adsorption of water on a hydrophobic surface - the case of antimony(111),* Chem. Phys. Lett., 517 (2011) 46-50, by J. Shan, A. Chakradhar, Z. Yu, U. Burghaus

Additional experimental details

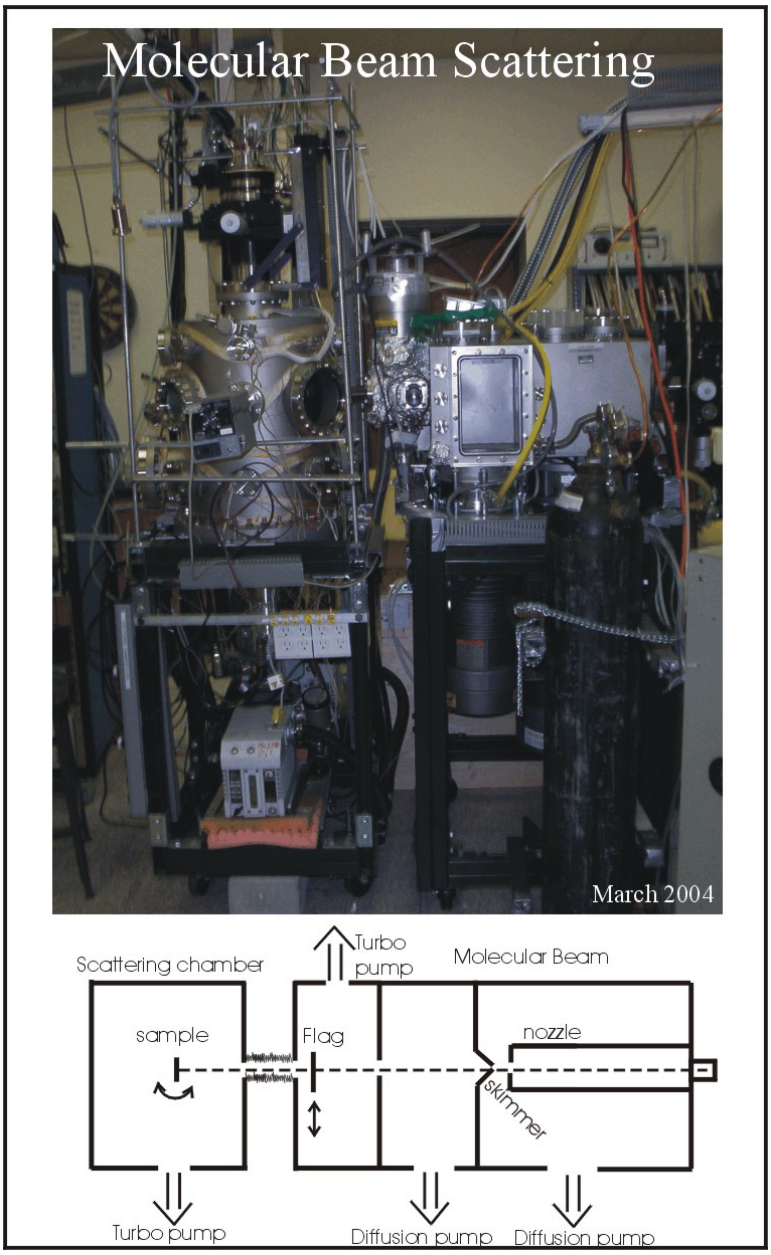

Fig. S12: Set-up of the molecular beam scattering system.

Experimental setup

The measurements have been performed with a home-built, triply-differentially pumped molecular beam system (**Fig. S12).**[10] The base pressure of the scattering chamber was $<2\times10^{-10}$ mbar. The supersonic beam is attached to a scattering chamber, which contains a

shielded mass spectrometer for thermal desorption spectroscopy (TDS) as well as an AES (Auger electron spectroscopy) and XPS (X-ray photoelectron spectroscopy) system. Water was dosed by backfilling as well as by a water molecular beam.

UHV TDS, ultra-high vacuum thermal desorption spectroscopy

The UHV TDS (ultra-high vacuum thermal desorption spectroscopy) technique may not be that well-known outside of the surface science community. Therefore, a typical measuring procedure is outlined in the following.

1) The sample is mounted inside a UHV vacuum chamber.

2) A mass spectrometer which simply measures the pressure of a given gaseous molecule in this vacuum chamber is mounted in close proximity to the sample.

3) The sample is cool down and subsequently e.g. a valve is opened to dose a gas in the vacuum chamber which adsorbs on the surface at low temperature. For the experiments described here water was dosed by backfilling as well as directly with a molecular beam scattering systems minimizing readsorption and pumping speed effects.

4) The surface temperature is increased and the pressure of a given gas detect simultaneously with the mass spectrometer.

Thus, TDS spectra depict simply the pressure of a given gaseous molecule vs. surface temperature. This pressure is related to the desorption rate. Thus, we obtain kinetics information since the higher the peak temperature the larger the binding energy of the probe molecule on the surface. Integrating the TDS curves quantifies the total amount of adsorbed species.

For TDS measurements on less conducting samples, electron bombardment heating is applied. The sample potential is ramped by means of a computer controlled high voltage (HV) power supply. Electrons evaporated from a W-filament, heated by means of a second computer

controlled power supply, are accelerated against the back of the surface. A homemade data acquisition program controls the heating ramp (T_s vs. time) by means of a software Proportional-Integral-Derivative (PID) controller, taking advantage of the real time clock of the PC. Since a combination of two power supplies is used, the total heating power is controlled via PID loop rather than the independent settings of the HV and filament current. In doing so, linear heating ramps can be obtained over a wide temperature range.

Literature survey

Graphene synthesis

Following well-established procedures,[11-20] we used transition metal single crystal surfaces as supports to grow graphene by physical vapor deposition (PVD). For example, the exposure of Ru(0001) (or other transition metals) to moderate pressures ($1x10^{-7}$ Torr) of ethylene, propylene, or benzene at 300 K, followed by annealing the sample at 1300 K, results in a partial graphene layer.[4, 5] Repeated cycles will fully cover the support. Similarly, dosing the hydrocarbon directly at high temperatures forms graphene.[20] Importantly, clean surface sites act as active sites to decompose hydrocarbon; that is, graphene growth is self-terminating, ensuring the formation of a single layer of carbon.[20] Graphene grows over step edges.[11-20] This is true for supports with low carbon solubility. The reduction of graphene oxide (chemical synthesis), segregation preparation with SiC and other supports, and physical techniques (mechanical exfoliation, e.g., the Scotch tape approach) have also been developed,[11-19] but are more challenging for a UHV model study. Graphene samples also are commercially available. However, studying these samples would require sample transfer through air which is problematic. See also section about sample characterization above.

Graphene support characterization

In case of Ru(0001), for example, LEED shows satellite peaks surrounding the hexagonal Ru(0001) support spots.[4, 5] In addition, the positive-to-negative ratio of the C-AES peak can be used to determine the graphene coverage.[4, 5] Chemical shifts have been seen in XPS. Thus, simple standard techniques, which are also available in our lab, allow one to verify the graphene layer formation. See also section about sample characterization above.

Why ruthenium?

Similar results have been obtained for other surfaces such as Ir and Rh.[17] However, the graphene structure on Ru is simpler than on other systems. For example, on Ir, bilayer formation has been seen due to carbon's high solubility in that system.[17] Other supports, including platinum, result in the formation of complex rotational domains.[17] Using supports that are less expensive than Ru would be interesting. However, on Ni, for example, commensurate graphene is formed, which prevents the use of standard LEED as a simple diagnostic technique. On Cu, high pressures of hydrocarbon are required, which is problematic in a UHV model study. In some cases only polycrystalline graphene is formed. Since our object is to explore the intrinsic properties of graphene, we specifically chose a simple procedure to obtain graphene. For our model study, ruthenium is the best system in this regard. We are aware of engineering type synthesis procedures as well as that graphene samples are even commercially available. However, our object is to characterize the intrinsic properties of graphene taking advantage of a UHV system.

Brief literature survey about water adsorption on graphene and ruthenium

General aspects of water adsorption properties on solid surfaces were reviewed e.g. in refs.[21-23]

Ruthenium. On Ruthenium which is used in this study as a support to grow graphene, water adsorption has been studied extensively[21-24] up to very recent works.[25] Explanations of unusual isotope effects and whether water dissociates or not, were discussed controversially. Latest density functional theory (DFT) studies conclude a partially dissociated hydroxyl-water overlayer.[25] However, isolated chemisorbed H_2O molecules should not dissociate. The traditional water bilayer structure is formed with the top layer not directly bound to the Ru surface.[25]

HOPG/experimental. Highly ordered pyrolytic graphite (HOPG) often serves as a reference system for carbon nanotubes and graphene. Perhaps amazingly, we could find only few experimental surface science studies about water adsorption even on HOPG.[26, 27] Accordingly, at low temperatures, water adsorbs nondissociatively on clean HOPG, forming hydrogen bonded aggregates.[26, 27] Despite that result, both experimental studies,[26, 27] employing basically the same experimental techniques, are in distinct disagreement.

The TDS data in ref.,[26] are dominated by one structure with an apparently coverage independent desorption rate. Thus, 0^{th} order kinetics is evident, down to submonolayer water coverages,[26] which is typically thought to occur for hydrophobic systems.[28] A two phase regime[26] or nanodroplets[29] may act as a reservoir for desorption, similarly to multilayers at large coverages. Therefore, the desorption rate becomes constant (coverage independent). In addition, from high resolution electron energy loss spectroscopy (HREELS), two-dimensional (2D) water cluster formation up to 0.5 ML was concluded.[26] Above 0.5 ML, 3D water clusters form. In contrast, contact angle measurements at ambient pressure indicated wettability of water with

clean HOPG.[26] Whether or not clean HOPG is strictly hydrophobic (nonwetting) remains somewhat unclear from this study. Hypothesized is that truly clean HOPG is not hydrophobic, judged by contact angle measurements.[26]

According to ref.,[27] various TDS peaks were detected and deviations from 0^{th} order kinetics was seen.[27] Here, the kinetics appears to be similar to non-hydrophobic systems were monolayer and multilayer structures can be distinguished in TDS.

In another recent study on water/HOPG, time-of-flight secondary ion mass spectrometry and TDS were utilized.[30] Three structures were seen in H_2O TDS,[30] somewhat similar to the data in ref.[27] (As a perhaps important detail, quite different cleaning/annealing temperatures were used in refs.[27, 30]: 500 K (not ultimately UHV clean HOPG) vs. 1200 K (UHV clean HOPG)) Also in this study[30] for a hydrophobic system unusual high wettability was concluded and attributed to the structure of the water layer (OH groups oriented towards the surface) which results in attractive water HOPG interactions.[30]

In a recent ambient pressure AFM study on HOPG, nanodroplets were seen (consistent with 0^{th} order kinetics down to small water coverages).[29] Defects acted as nucleation sites for these droplets. The HOPG surface was, however, not cleaned in this ambient pressure study.

A few more experimental works on water coadsorption systems and photon induced processes can be found for HOPG.

Thus, quite controversial data and interpretations are evident in the literature even for the traditional HOPG system, see also the tables given below.

HOPG/theoretical. Water physisorbes with no changes induced on the HOPG surface, according to ref.[31] No adsorption site or molecular orientation preference was seen theoretically for small H_2O coverages. At large concentrations, configurations with molecular dipoles parallel

to the surface plane were energetically favored.[31] Even on defected graphite water appears to adsorb molecularly, only on specific defects dissociation was seen with large activation energies.[32]

Graphene/experimental. To the best of our knowledge, the water/graphene system has not been characterized experimentally at UHV. Experimental works focuses on ambient pressure experiments such as contact angle measurements, Raman spectroscopy, optical microscopy, etc. Although studies are often supported by theoretical works, very divers conclusions can be found.[33]

In ref.[34] it was concluded that a single graphene layer does not alter the wetting properties of certain supports such as copper and gold ("wetting transparency of graphene"). For thick layer, contact angles similar to bulk graphite were obtained. Thus, thick carbon layers or HOPG are hydrophobic. Graphenes wettability depends on the support's wettability. All the prior experiments in ref.[34] were conducted, however, at ambient pressure. Molecular dynamics (MD) simulations[34] supported these conclusions. Accordingly, the water adsorption energy decreases with carbon layer thickness and the contact angle increases. As a plausible reasoning the authors state that the thinness of the graphene layer does not affect significantly the number of neighbours (and interactions). Although plausible, for the Ruthenium support used in our study, this model[34] would predict wettability and hydrophilic properties for graphene/ruthenium. Thus, at least two TDS peaks and none-zero order water TDS kinetics would be expected. This is in contrast to our experiments.

A similar study based on ambient pressure contact angle measurements and MD simulations concludes that graphene is not entirely transparent to wetting.[35] Wetting transparency

breaks down for super-hydrophobic/hydrophilic substrates which are quite extreme cases.[35] Therefore, refs.[34, 35] appear conceptually consistent.

In ref.[36] again, ambient pressure contact angle measurements and MD simulations were presented, but result in conclusions directly diametric to refs.[34, 35]. In this study, a negligible effect of the support is concluded. A contact angle of 93° (poor wetting, hydrophobic) was determined for graphene independent of the support and graphene layer thickness.[36] Our UHV TDS data appear qualitatively in agreement with these findings.

All of these studies were published in the highest impact factor journals.

Using apparently the same experimental and theoretical techniques the conclusions range from "wetting transparency of graphene"[34] over "not entirely transparent to wetting"[35] to "negligible effect of the support".[36]

Graphene/theoretical. Most literature about water-graphene interactions is purely theoretically or rather applied. In contrast to carbon nanotubes were nanoconfined water adsorption is characterized in very detail,[16] to the best of our knowledge, experimental ultra-high vacuum (UHV) surface science projects have not been published for water/graphene.

For molecular dynamics (MD) simulations predict a wetting transparency of graphene, see ref.[34]; for MD simulations predicting that graphene is not entirely transparent to wetting see ref.[35]

Why study water/graphene? Water/HOPG has been studied experimentally in some detail before. Therefore, is it useful at all to consider water/graphene?

First, the support used to grow epitaxial graphene may affect the electronic structure of the graphene layer. HOPG is not graphene. Second, in DFT/vdW studies it was explicitly seen that binding energies on graphite are larger than on graphene due to the long-range character of

van der Waals interactions.[37, 38] HOPG is apparently intrinsically non-hydrophobic, based on experimental works. The water/graphene interaction is basically experimentally uncharacterized. It is experimentally unknown whether graphene is intrinsically hydrophobic or not. Obviously, the nanoscience of 2D graphite is very different than properties of 3D bulk HOPG. Therefore, a priori it is unclear whether adsorption kinetics of adsorbates on HOPG are also valid for graphene. From a practical perspective, in catalysis, water graphite interactions are of some interest in the coal gasification process.[39] Some graphene devises are based on changes in electrical conductivity due to interaction with gas-phase molecules. The lubrication properties of graphite are affected by water moisture.[40] And, of course, graphene is an exciting new material.

Water/CNTs. A literature survey can be found in ref.[16] Most fundamental science studies focus on the structure of water ice in CNTs.

Indications for strictly zeroth order kinetics

Considering TDS data, visual inspection of the desorption traces should show the following.

- In data sets of different initial coverage, low temperature edges line up
- Low temperature edges increase exponentially with temperature
- TDS peaks do not saturate with increasing exposure, TDS intensities go up for ever
- Low overall desorption temperatures
- Sharp drop to zero of the high temperature edges (may be affected by pumping speed and readsorption)

Standard conclusions from these observations

- (Near) zero desorption order
- Water binds more strongly to itself (via hydrogen bonding) than to the support
- 3D island formation at low exposures

Contact angles and wettability

The following definition is commonly used for ambient pressure studies.

Contact angle	**Degree of wetting**
$\theta = 0$	Perfect wetting
$0 < \theta < 90°$	High wettability
$90° \leq \theta < 180°$	Low wettability, poor wettability
$\theta = 180°$	Perfectly non-wetting, hydrophobic

Further data tables

Ultra-high vacuum kinetics studies					
System	**Hydrophobic**	**0th order kinetics?**	**Number of TDS peaks**	**Method**	**Ref.**
Au(111)	Yes	Yes	1	UHV, TDS	41
O_2-Au(111)	Yes	Yes	1	UHV, TDS	42
D_2-Ni(111)	Yes	Yes	1	UHV, TDS	39
D_2-Pt(533)	Yes	Yes	1	UHV, TDS	43
Octane-Pt(111)	Yes	Yes	1	UHV, TDS	44
Water-Pt(111)	Yes	Yes	1	UHV, TDS	45
Antimony(111)	Yes	Yes	1	UHV, TDS	28
Cu(111)	Yes	Yes	1	UHV, TDS	46
Ag(011)		Yes	---	HREELS	47
silver					48
HOPG	No*	No	4	UHV, TDS	27
HOPG	No	Yes	1	UHV, TDS	26
HOPG	No*	No	3	UHV, TOF-SIMS, TDS	30
A few other studies on graphitic systems					
HOPG	Yes	---		Ambient, contact angle	26
HOPG	Yes			Ambient, AFM	29

Adsorption energy of water	**System / method**	**Ref.**
12.8 kJ / mol	HOPG / DFT-cc	[38]
14.6 kJ / mol	Graphene / DFT-cc	[38]
0.45 ± 0.03 eV/molecule	HOPG / TDS	[26]
39.9 ± 0.8 kJ/mol	HOPG / TDS	[27]
43.4 ± 2.9 kJ/mol	Sublimation enthalpy of ice	From ref.[27]
0.49 eV/molecule	Sublimation enthalpy of ice	From ref. [26]

1eV = 8065.6 cm^{-1}
1eV = 96.485 kJ/mol

Preexponential factor	**System / method**	**Ref.**
$9x10^{25} – 1x10^{27}$ Molecules/(m^2s)	HOPG / TDS	[27]
10^{30} Molecules/(cm^2s)		[27]

Desorption order	**System / method**	**Ref.**
0.26 ± 0.02	HOPG / TDS	[27]
0	HOPG / TDS	[26]

References

1. A. Chakradhar, K.M. Trettel ,U. Burghaus, Chemical Physics Letters 590 (2013) 146-152
2. B. Borca , e. al, New J. Phys. 12 (2010) 093018
3. L. Liu, Z. Zhou, Q. Guo, Z. Yan, Y. Yao ,D.W. Goodman, Surf. Sci. 605 L47-L50
4. Y. Xu, L. Semidey-Flecha, L. Liu, Z. Zhou ,D.W. Goodman, Faraday Discuss. 152 (2011) 267
5. Z. Zhou, F. Gao ,D.W. Goodman, Surface Science 604 (2010) L31–L38
6. M. Komarneni, A. Sand, J. Goering, U. Burghaus, M. Lu, M. Veca ,Y.-P. Sun, Chem. Phys. Lett. 476 (2009) 227-231
7. M.S. Dresselhaus, A. Jorio ,R. Saito, Annu. Rev. Condens. Matter Phys. 1 (2012) 89–108
8. J. Goering, E. Kadossov, U. Burghaus, Z.Q. Yu, S. Thevuthasan ,L.V. Saraf, Catalysis Letters 116 (2007) 9
9. X. Feng, S. Maier ,M. Salmeron, J. Am. Chem. Soc. 134 (2012) 5662-5668
10. J. Wang , U. Burghaus, Journal of Chemical Physics 123 (2005) 184716
11. J. Wintterlin , M.L. Bocquet, Surf. Sci. 603 (2009) 1841-1852
12. D.S. Sua, S. Perathoner ,G. Centi, Catalysis Today 186 (2012) 1-6
13. A.L. Dicks, Journal of Power Sources 156 (2006) 128-141
14. J.M. Planeix, N. Coustel, B. Coq, V. Brotons, P.S. Kumbhar, R.D. Utartre, P.G. Eneste, P.B. Ernier ,P.M. Alayan, J. Am. Chem. Soc. 116 (1994) 7935
15. A.V. Melechko, V.I. Merkulov, T.E. McKnight, M.A. Guillorn, K.L. Klein, D.H. Lowndes ,M.L. Simpson, Journal of Applied Physics 97 (2005) 041301/1-041301/39
16. U. Burghaus, (2009) Gas-carbon nanotubes interactions: a review of ultra-high vacuum surface science studies on CNTs, in Carbon nanotubes - Research Trends, Nova Science (New York), ISBN 978-1-60692-236-1
17. M. Batzill, Surface Science Reports 67 (2012) 83–115
18. T.O. Wehling, M.I. Katsnelson ,A.I. Lichtenstein, Chemical Physics Letters 476 (2009) 125–134
19. C. Oshimay , A. Nagashima, J. Phys.: Condens. Matter 9 (1997) 1-20
20. K. Donner , P. Jakob, THE JOURNAL OF CHEMICAL PHYSICS 131 (2009) 164701
21. P.A. Thiel , T.E. Madey, Surface Science Reports 7 (1987) 211
22. M.A. Henderson, Surface Science Reports 46 (2002) 1
23. R.S. Smith , B.D. Kay, Surface Review and Letters 4 (1997) 781
24. P.J. Schmitz, J.A. Polta, S.L. Chang ,P.A. Thiel, Surface Science 186 (1987) 219-231
25. A. Michaelides, A. Alavi ,D.A. King, J. AM. CHEM. SOC. (2003) 2746-2755
26. D.V. Chakarov, L. Osterlund ,B. Kasemo, Langmuir 11 (1995) 1201-1214
27. A.S. Bolina, A.J. Wolff ,W.A. Brown, Journal of Physical Chemistry B 109 (2005) 16836-16845
28. J. Shan, A. Chakradhar, Z. Yu ,U. Burghaus, Chem. Phys. Lett. 517 (2011) 46-50
29. P. Cao, K. Xu, J.O. Varghese ,J.R. Heath, Nano Lett. 11 (2011) 5581-5586
30. R. Souda, J. Phys. Chem. C 116 (2012) 20895−20901
31. P.C. Sanfelix, S. Holloway, K.W. Kolasinski ,G.R. Darling, Surface Science 532-535 (2003) 166-172
32. S.C. Xu, S. Irle, D.G. Musaev ,M.C. Lin, J. Phys. Chem. C 111 (2007) 1355-1365
33. editorial, Nature Materials 12 865
34. J. Rafiee, X. Mi, H. Gullapalli, A.V. Thomas, F. Yavari, Y. Shi, P.M. Ajayan ,N.A. Koratkar, Nature Materials 11 (2012) 217
35. C.J. Shih, Q.H. Wang, S. Lin, K.C. Park, Z. Jin, M.S. Strano ,D. Blankschtein, Phys. Rev. Lett. 109 (2012) 176101
36. R. Raj, S.C. Maroo ,E.N. Wang, Nano Lett. 13 (2013) 1509-1515
37. A. Ambrosetti , P.L. Silvestrelli, J. Phys. Chem. C 115 (2011) 3695-3702
38. J. Kysilka, M. Rube, L. Grajciar, P. Nachtigall ,O. Bludsk,
39. J. Shan, J.F.M. Aarts, A.W. Kleyn ,L.B.F. Juurlink, Phys. Chem. Chem. Phys. 10 (2008) 4994–5003
40. A. Ambrosetti, J. Phys. Chem. C 117 (2013) 321−325
41. B.D. Kay, K.R. Lykke, J.R. Creighton ,S.J. Ward, J.Chem.Phys. 91 (1989) 5120-5221
42. R.G. Quiller, T.A. Baker, X. Deng, M.E. Colling, B.K. Min ,C.M. Friend, J. Chem. Phys. 129 (2008) 064702
43. M.J.T.C.v.d. Niet, I. Dominicus, M.T.M. Koper ,L.B.F. Juurlink, Phys. Chem. Chem. Phys. 10 (2008) 7169-7179
44. T.R. Linderoth, V.P. Zhdanov ,B. Kasemo, Phys. Rev. Lett. 90 (2003) 156103
45. G.A. Kimmel, N.G. Petrik, Z. Dohnalek ,B.D. Kay, Phys. Rev. Lett. 95 (2005) 166102
46. B.J. Hinch , L.H. Dubois, J. Chem. Phys. 96 (1992) 3262

47. K.J. Wu, L.D. Peterson, G.S. Elliott ,S.D. Kevan, J. Chem. Phys. 91 (1989) 7964
48. A. Michaelides , K. Morgenstern, Nature Materials 6 (2007) 597